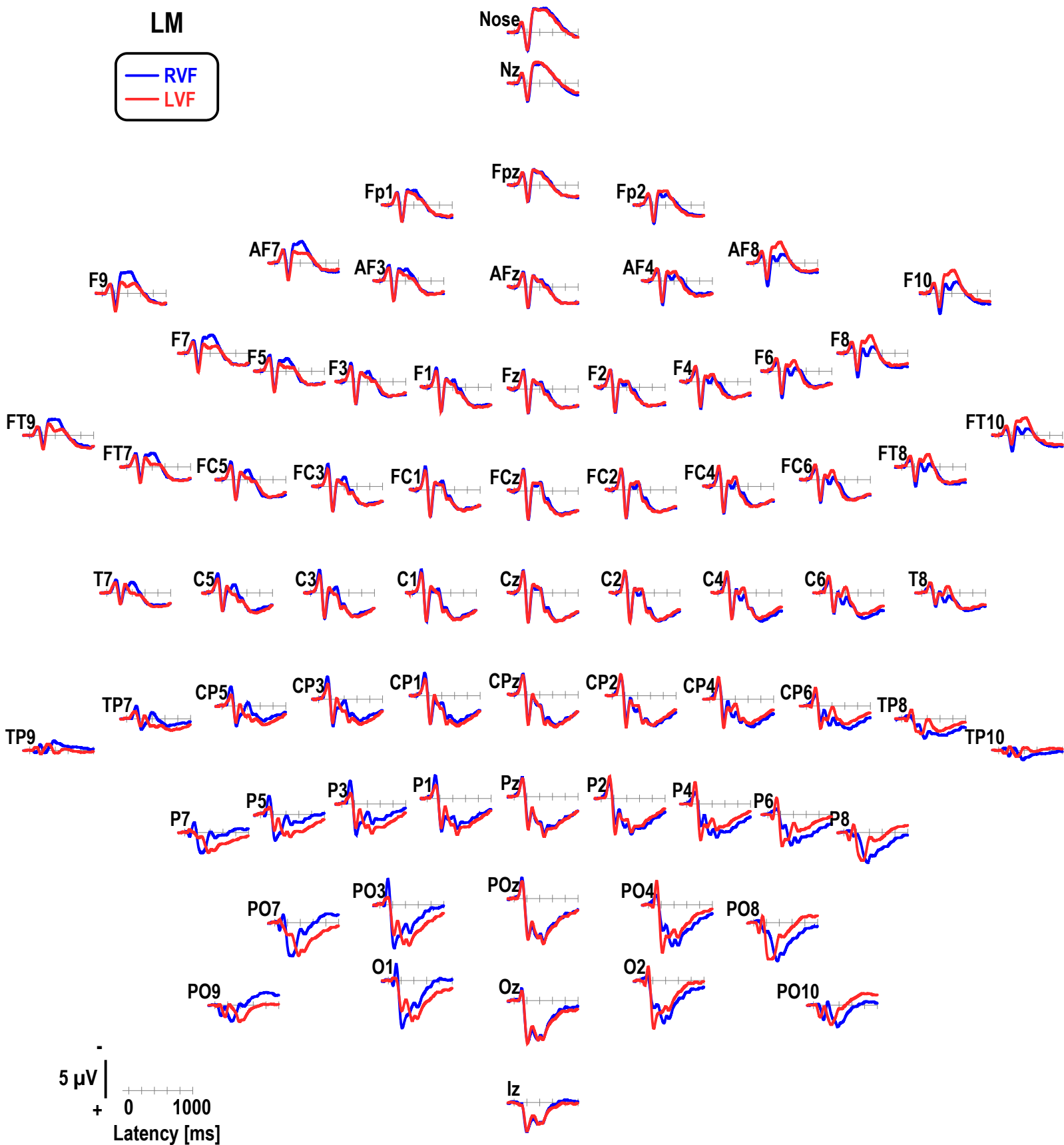
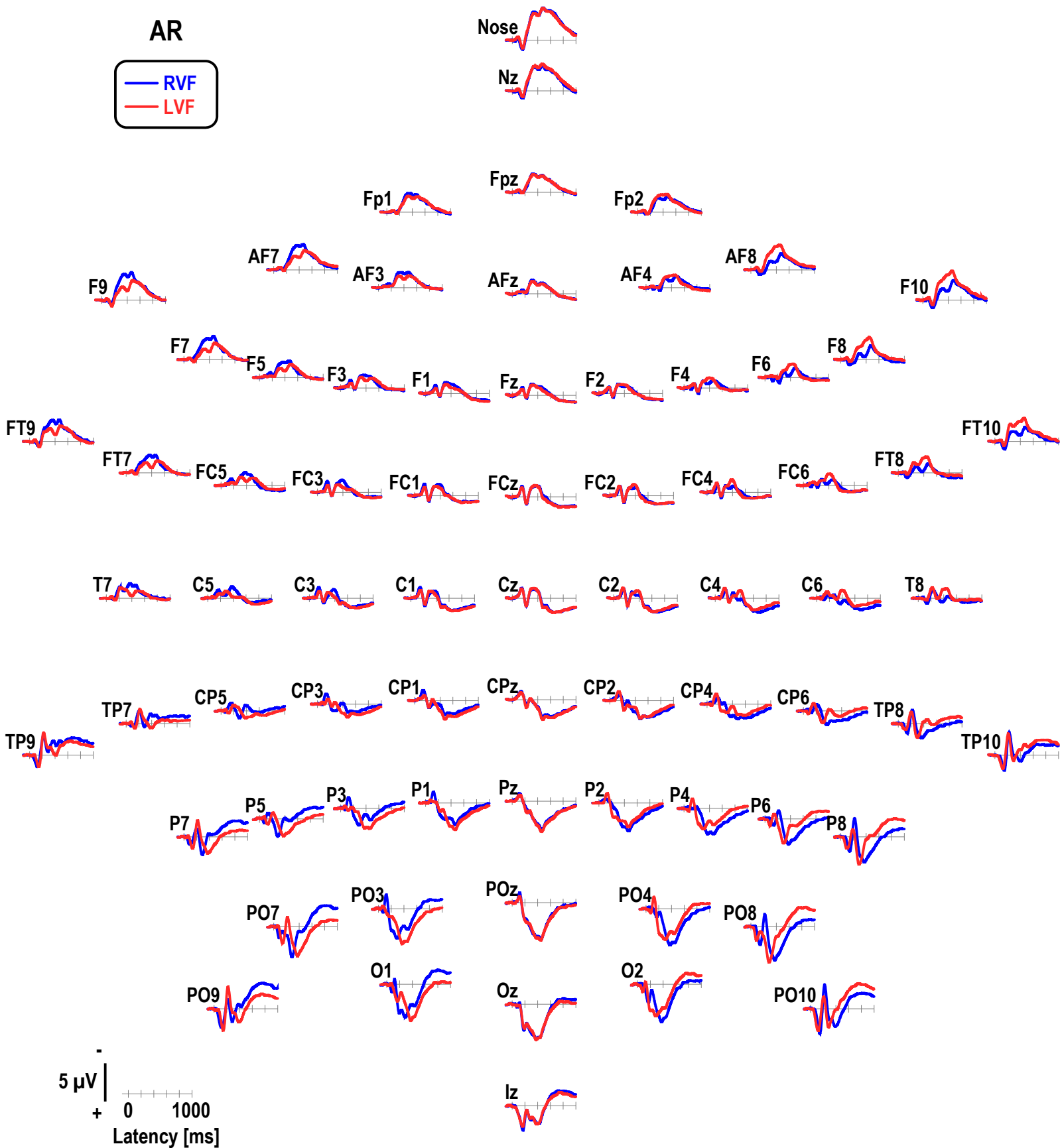


**Fig. S1.** Nose-referenced (NR), grand mean event-related surface potential (ERP) [ $\mu\text{V}$ ] waveforms (–100 to 1000 ms, 100 ms prestimulus baseline) for left and right visual field presentations at all 72 recording sites. Horizontal and vertical electrooculograms (EOG) are shown before blink correction.



**Fig. S2.** ERPs shown in Fig. S1 referenced to linked mastoids (LM; sites TP9 and TP10).



**Fig. S3.** ERPs shown in Fig. S1 referenced to all 72 recording sites (AR; average reference).

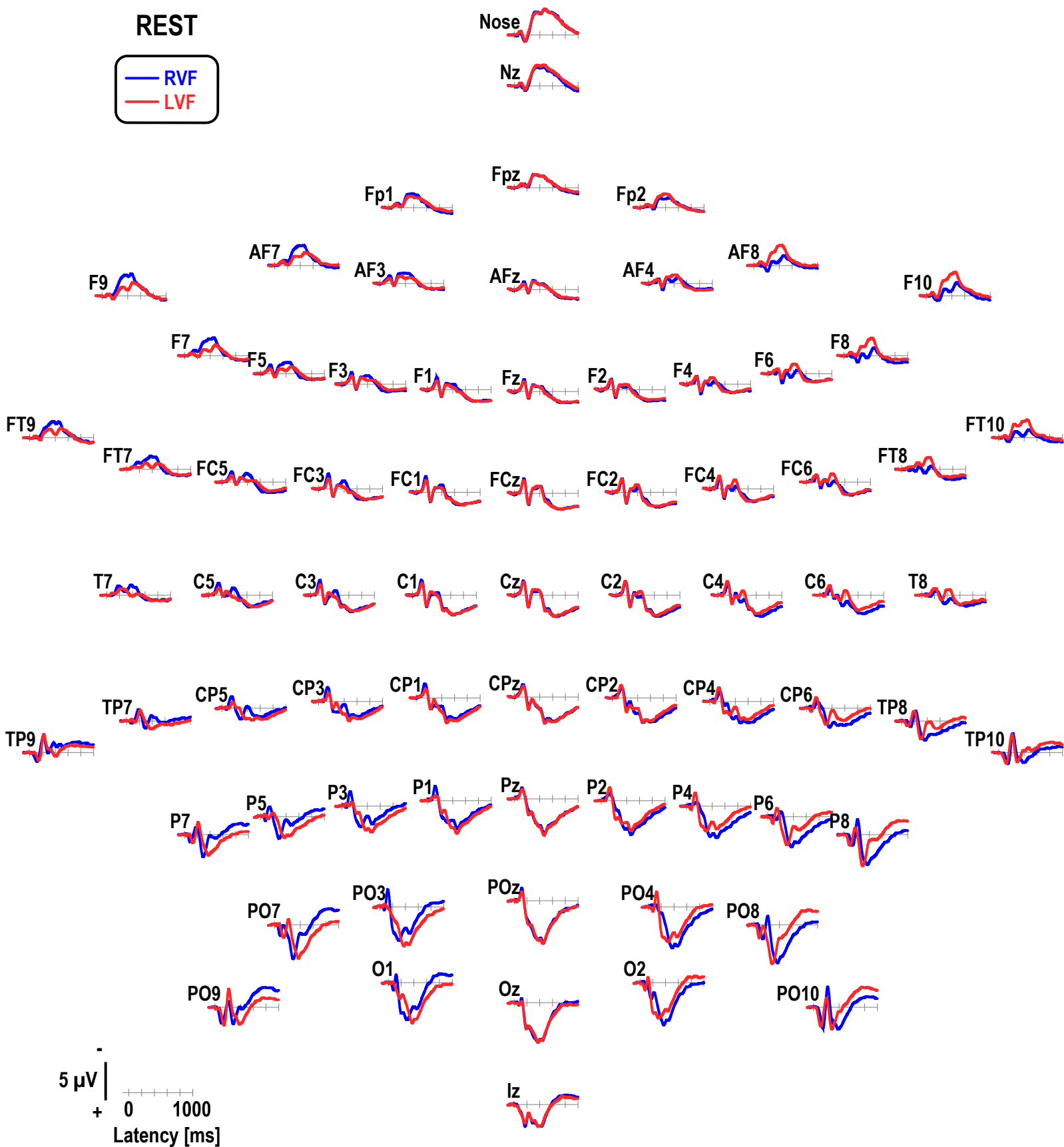


**Fig. S4.** ERPs shown in Fig. S1 referenced to infinity (REST; reference electrode standardization technique; Yao, 2001).

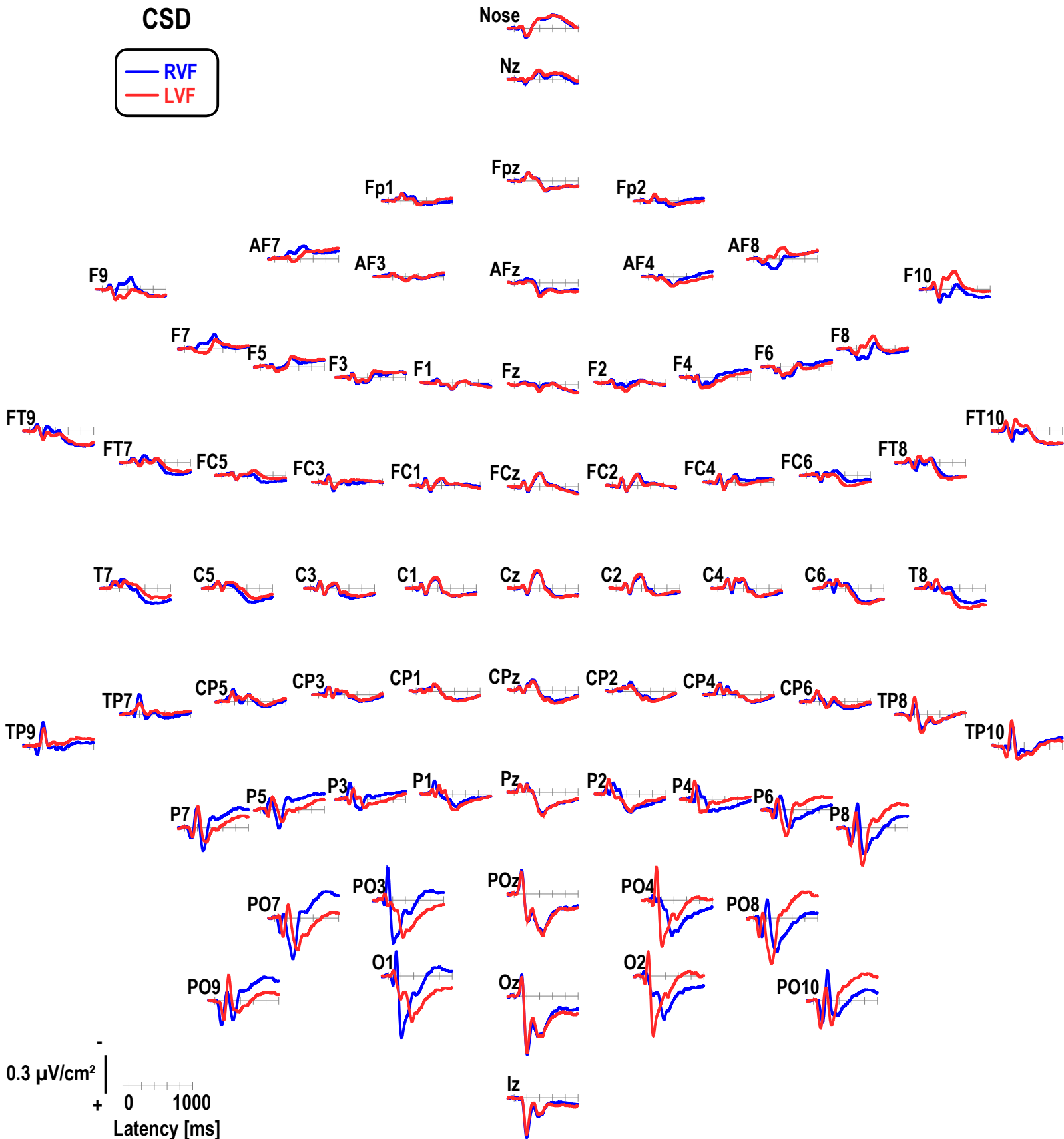


**Fig. S5.** ERPs shown in Fig. S1 transformed to current source density (CSD) [ $\mu\text{V}/\text{cm}^2$ ] waveforms using a spherical spline surface Laplacian interpolation ( $m = 4, \lambda = 10^{-5}$ ; Perrin et al., 1989).

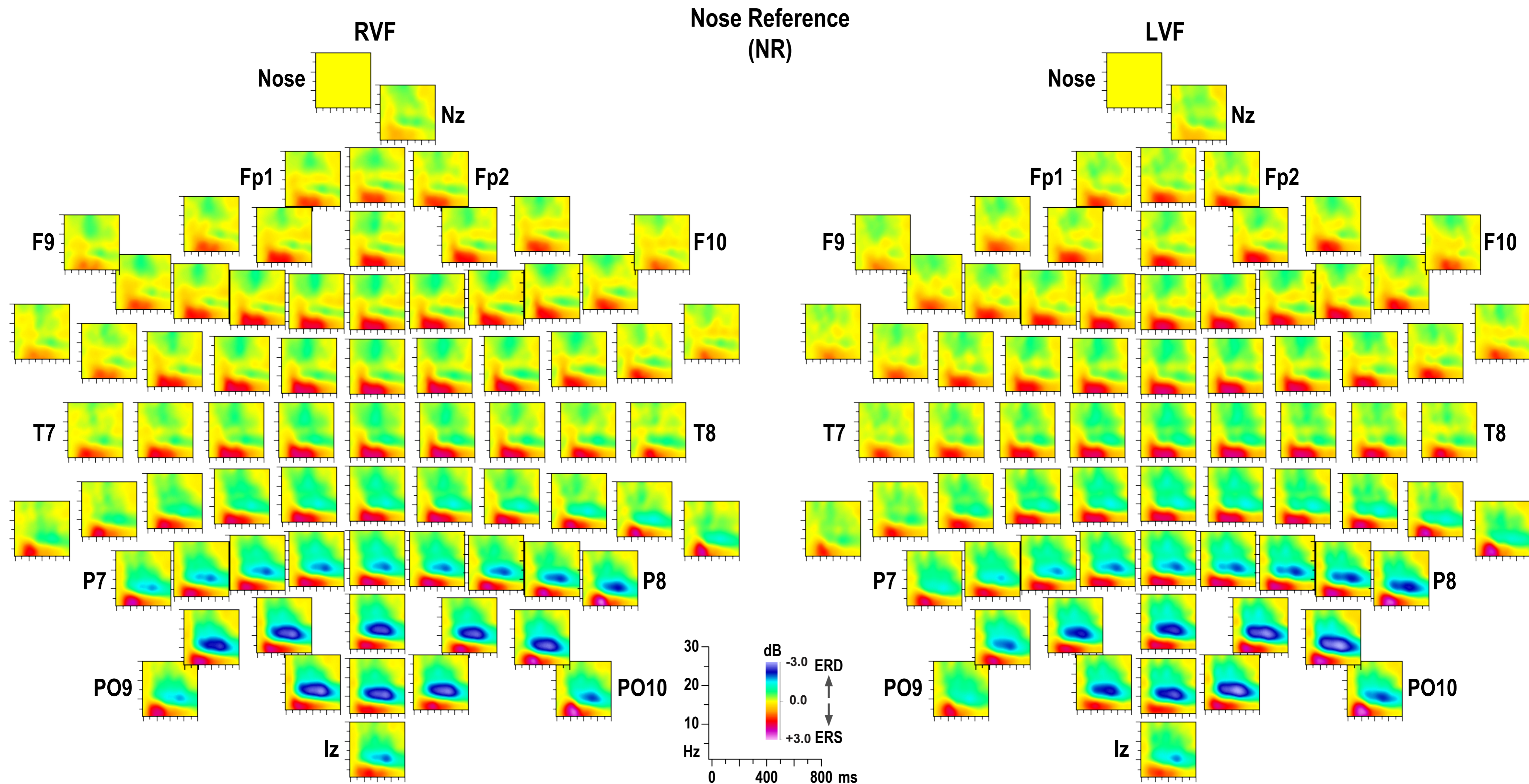


**Fig. S6.** Grand mean event-related spectral perturbation (ERSP) plots (0 to 800 ms; 1 to 30 Hz) for left and right visual field presentations at all 72 recording sites using nose-referenced (NR) EEG.

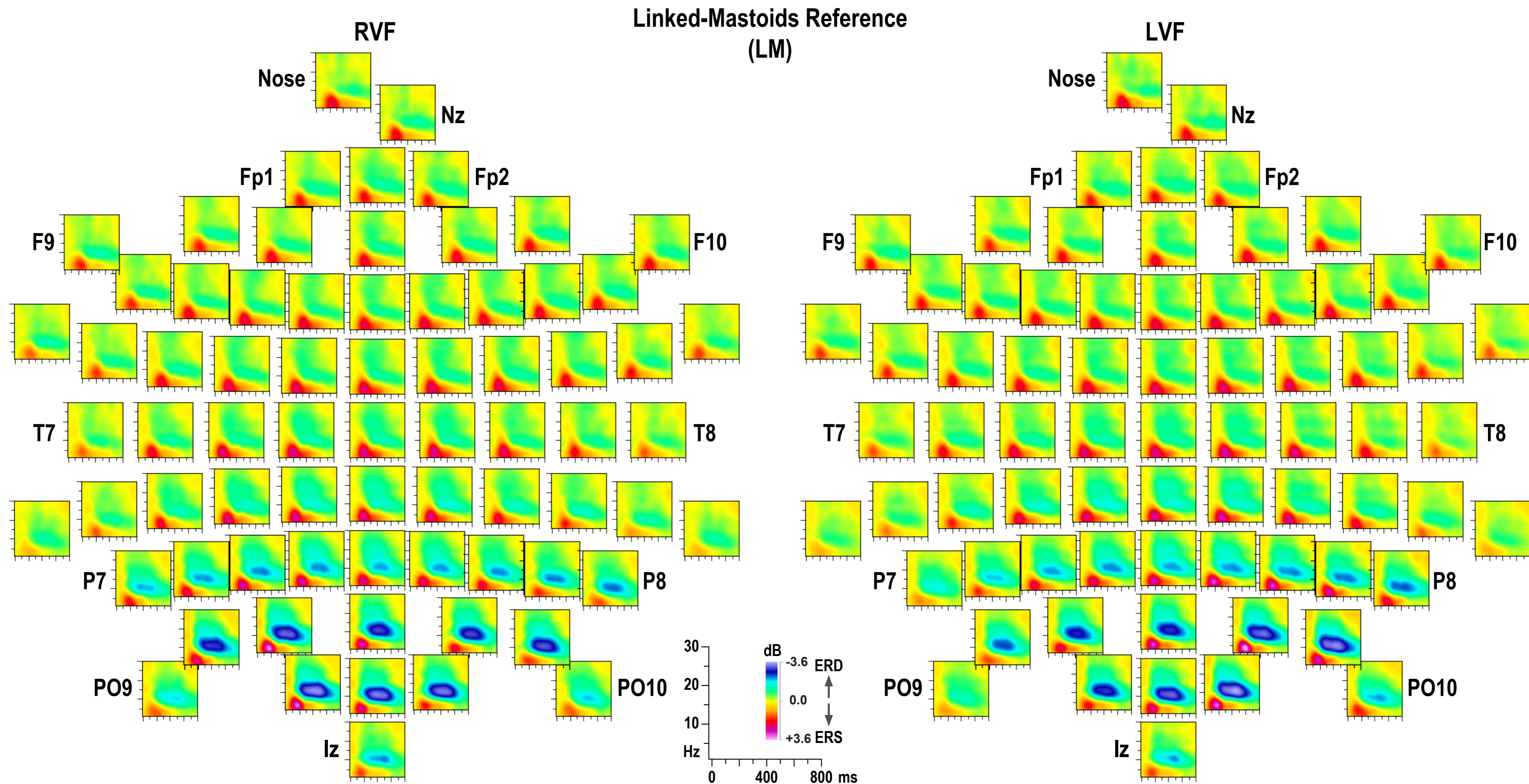


**Fig. S7.** ERSPs as shown in Fig. S6 using EEG referenced to linked mastoids (LM; sites TP9 and TP10).

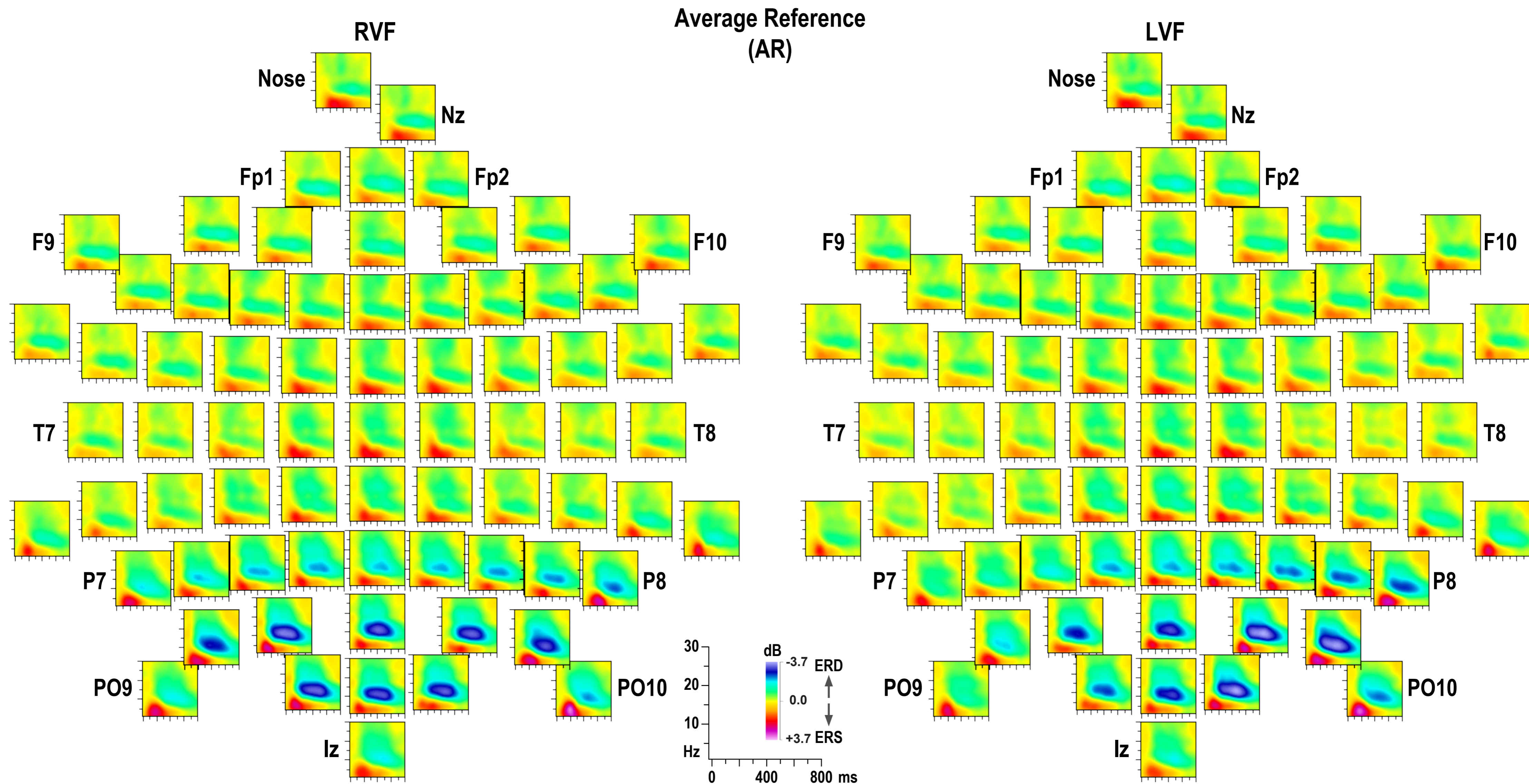


**Fig. S8.** ERSPs as shown in Fig. S6 using EEG referenced to all 72 recording sites (AR; average reference).

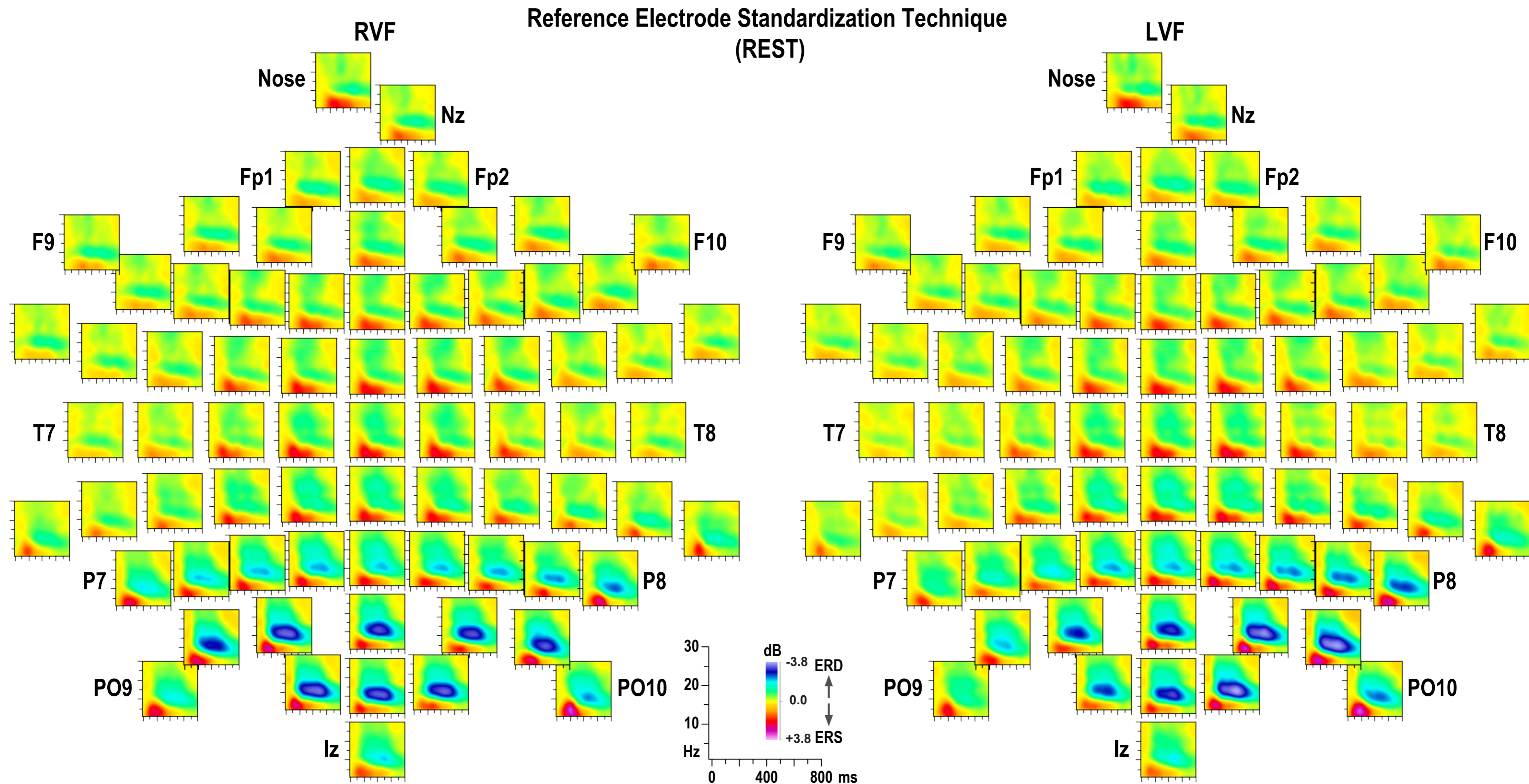


**Fig. S9.** ERSPs as shown in Fig. S6 using EEG referenced to infinity (REST; reference electrode standardization technique; Yao, 2001).

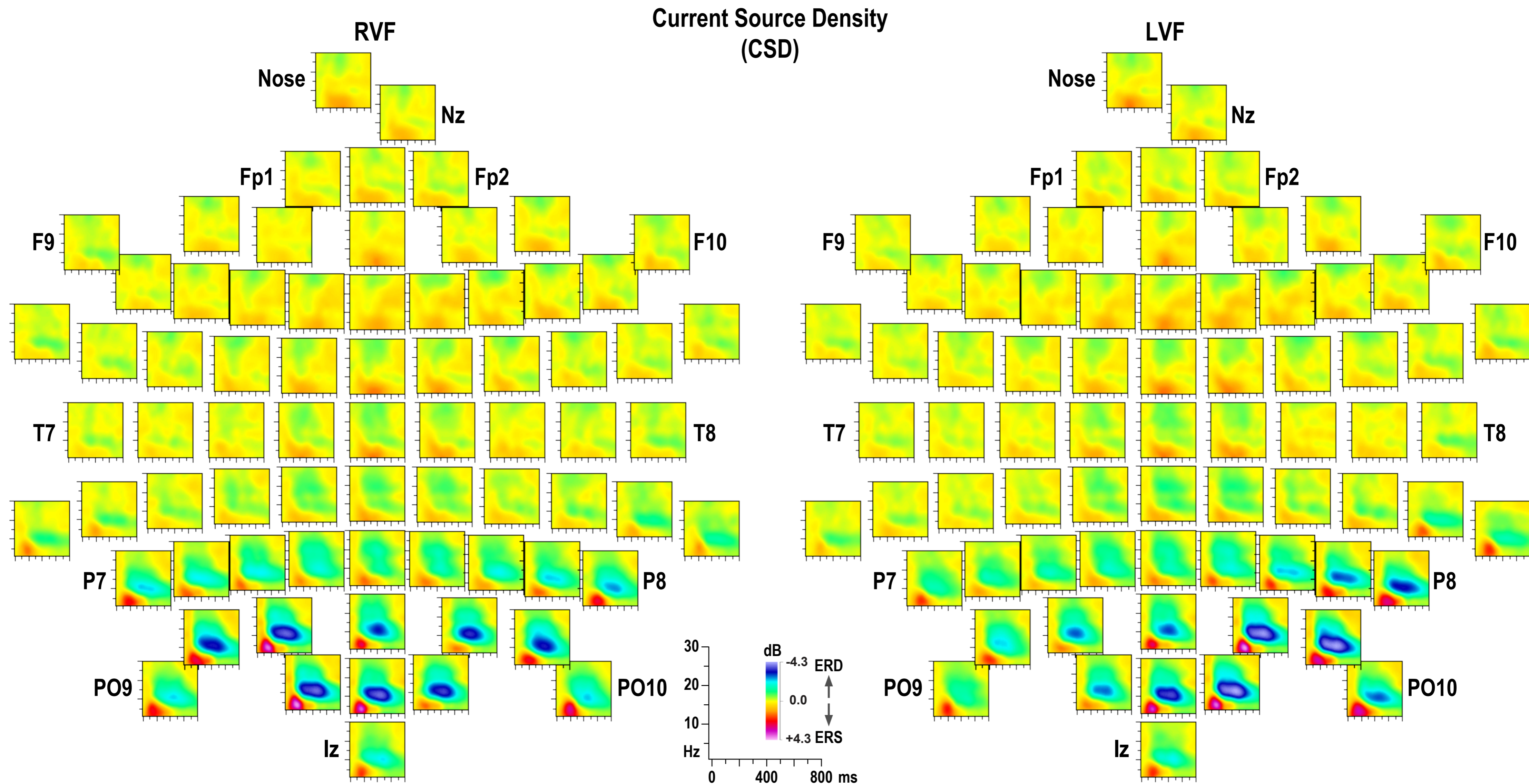


**Fig. S10.** ERSPs as shown in Fig. S6 using EEG transformed into current source density (CSD) [ $\mu\text{V}/\text{cm}^2$ ] via a spherical spline surface Laplacian interpolation ( $m = 4, \lambda = 10^{-5}$ ; Perrin et al., 1989).

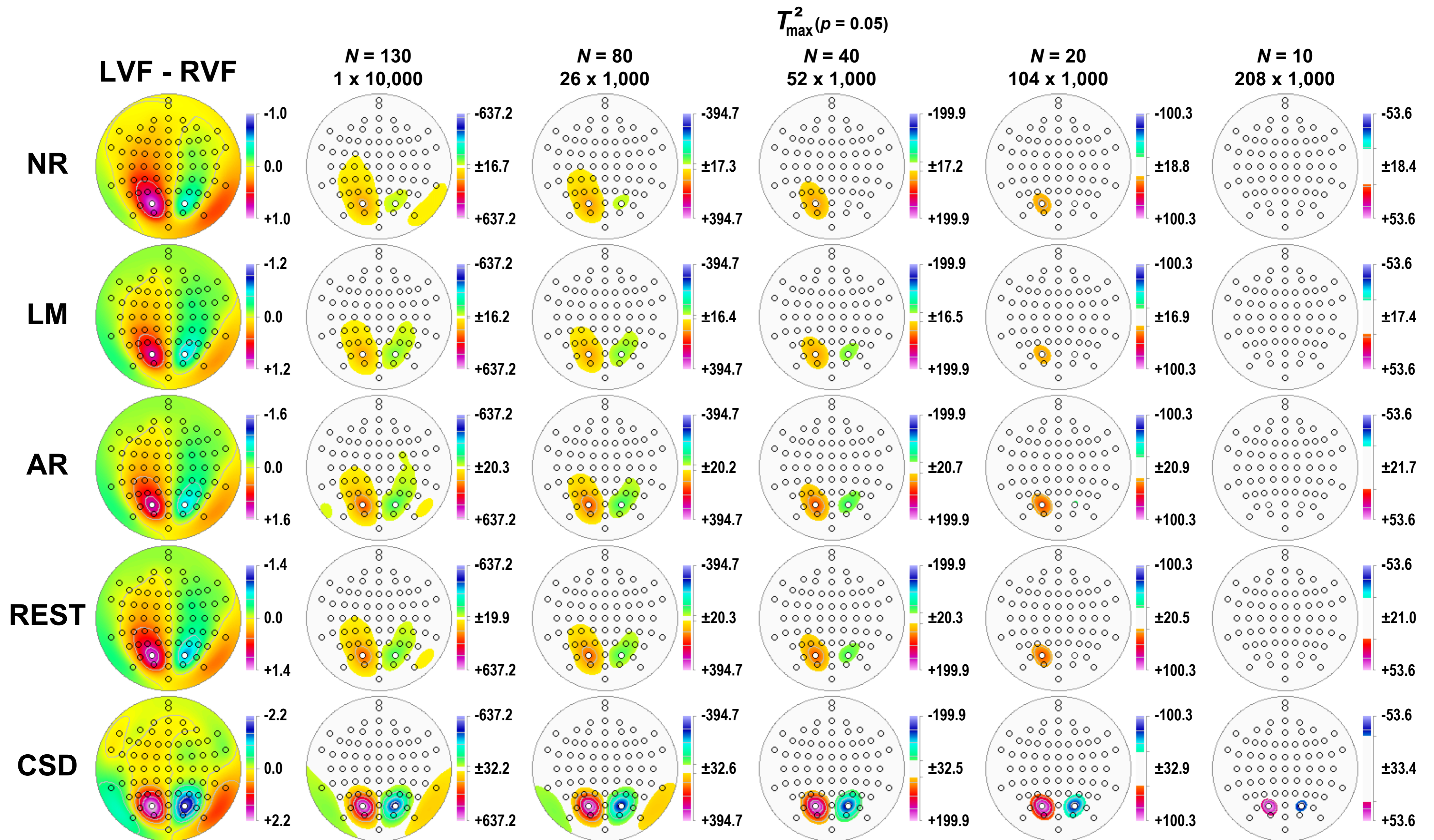


**Fig. S11.** Statistical evaluation of topographic visual field effects of factor 127 (N1) as in Fig. 4, comparing the randomization tests for the full sample ( $N = 130$ ; 10,000 repetitions) with those for randomly selected subsamples ( $N = 80$ , 26 draws;  $N = 40$ , 52 draws;  $N = 20$ , 108 draws;  $N = 10$ , 208 draws; 1000 repetitions each). Shown are for each data transformation the mean factor score difference topographies (i.e., left [LVF] minus right [RVF] hemifield) and corresponding  $\max(T^2)$  topographies thresholded at the 95<sup>th</sup> quantile ( $p = 0.05$ ). For subsamples, mean  $T^2$  statistics were evaluated with the cumulative randomization distribution resulting from the product of draws and repetitions.

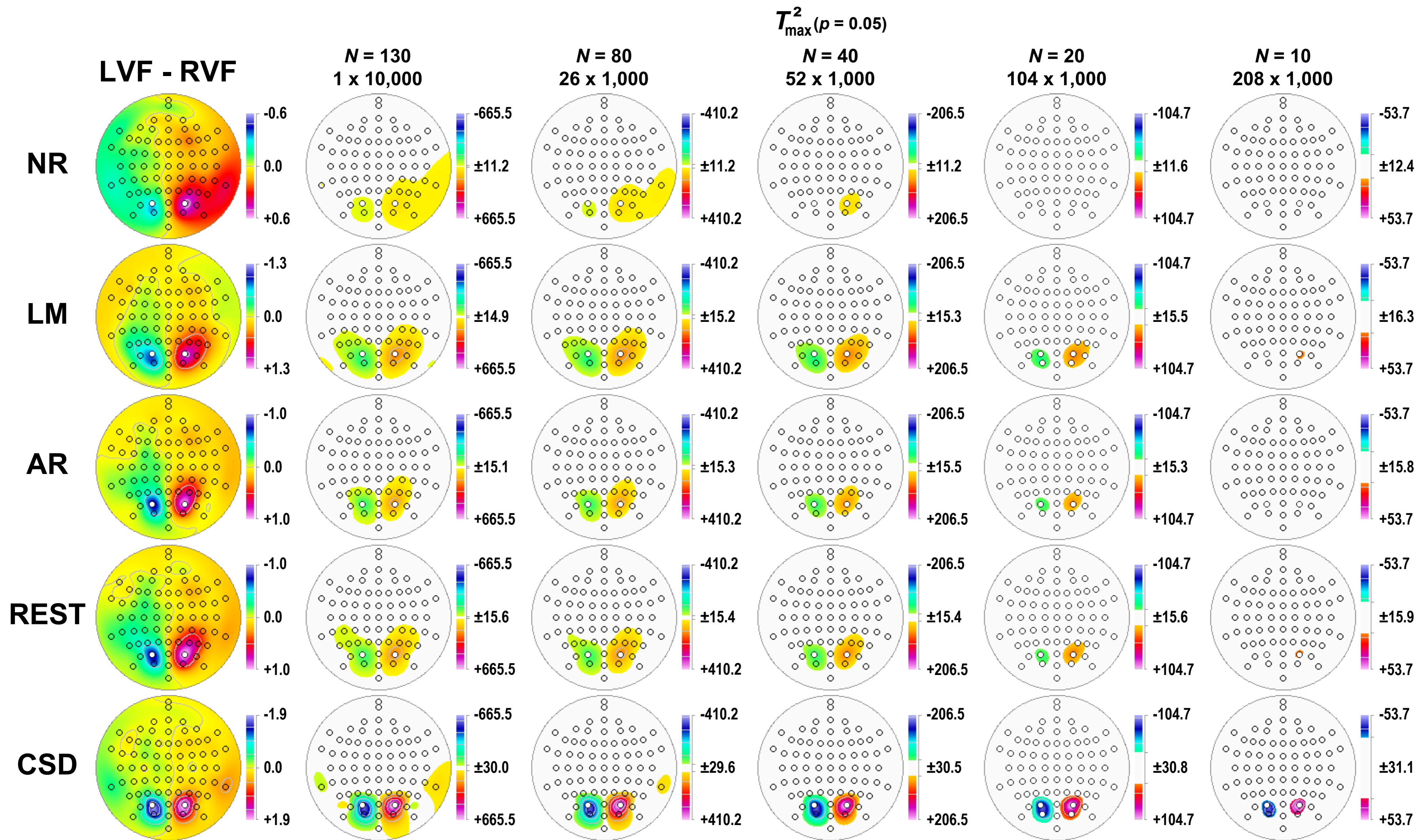


**Fig. S12.** Statistical evaluation of topographic visual field effects of factor 160-4 (N1 delta ERS) as in Fig. S11.

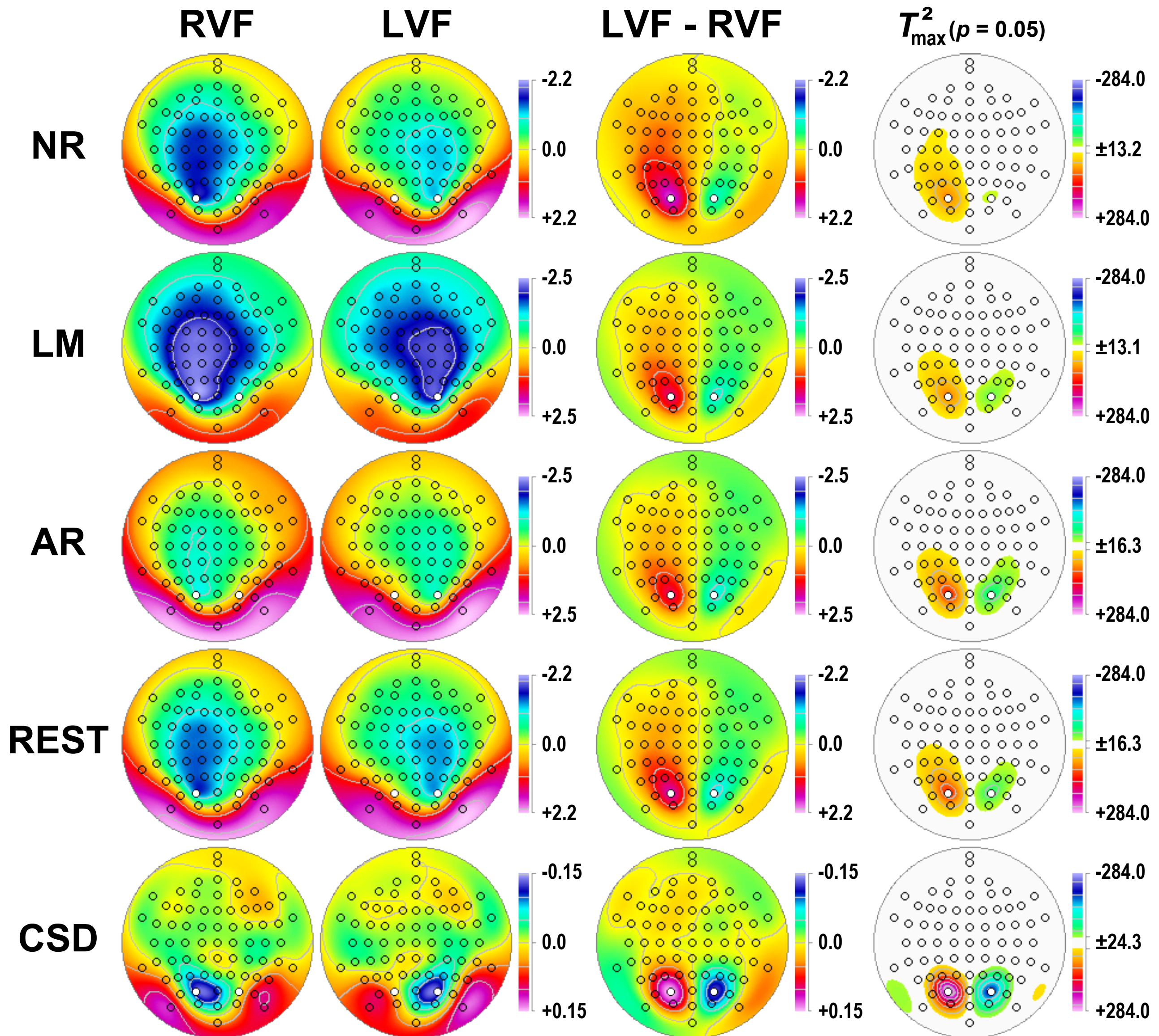


**Fig. S13.** Statistical evaluation of topographic visual field effects of N1 amplitude (time window 90–160 ms) as in Fig. 4.

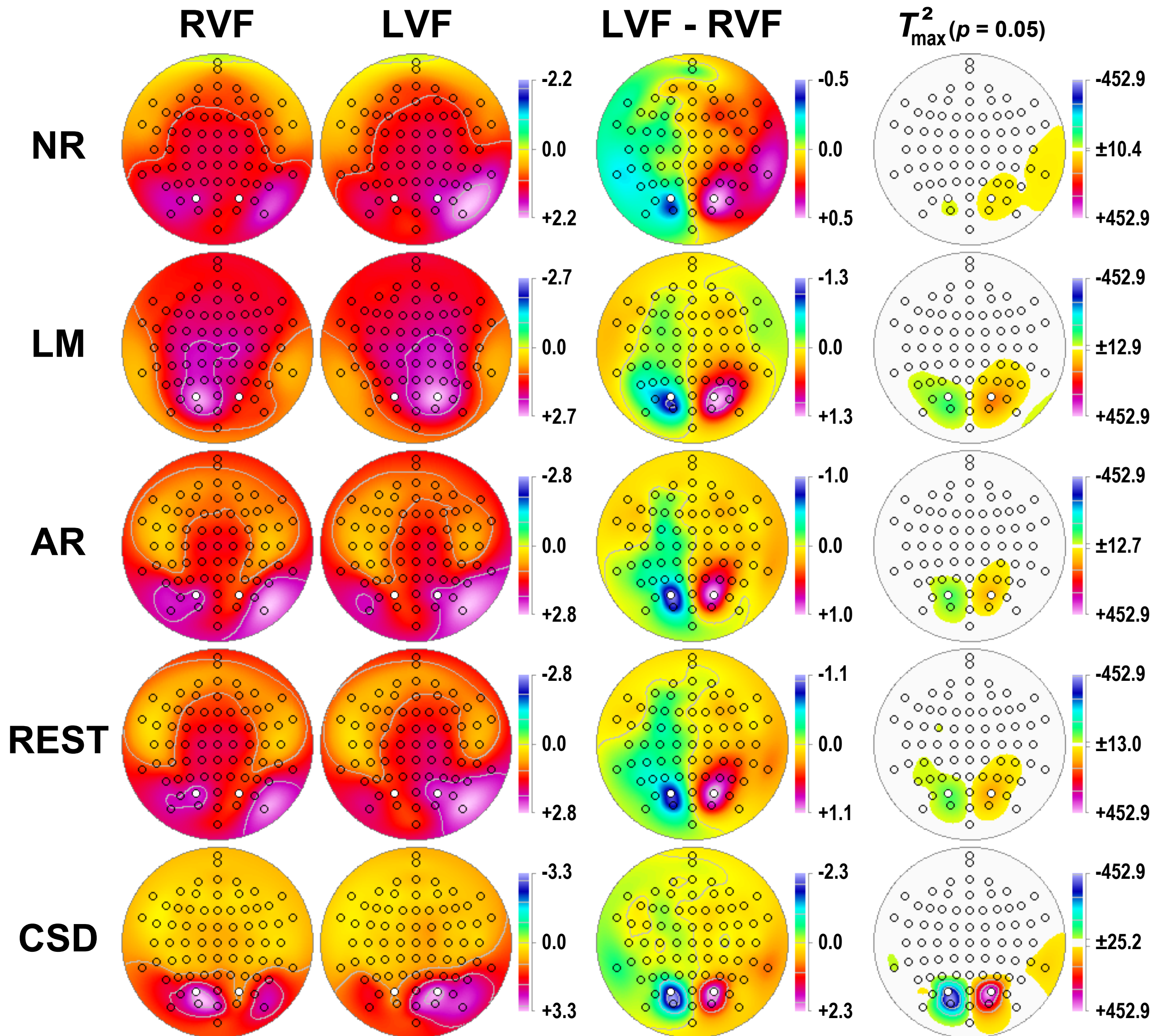


**Fig. S14.** Statistical evaluation of topographic visual field effects of N1 delta ERS (time-frequency-window 100–250 ms/2–6 Hz) as in Fig. 7.